Program Digest, 2019 IEEE International Ultrasonics Symposium (IUS)
Glasgow, Scotland, October 6-9, 2019

Lesion Imaging and Target Detection in Complex Heterogeneous Media: Application to Lung Nodules

Kaustav Mohanty
Dept. of Mechanical and Aerospace Engineering
NC State University, Raleigh, U.S.A
kmohant@ncsu.edu

John Blackwell
Div. of Cardiothoracic Surgery, Dept. of Surgery
University of North Carolina, Chapel Hill, U.S.A
johnwm@email.unc.edu

Mir Ali
Div. of Cardiothoracic Surgery, Dept. of Surgery
University of North Carolina, Chapel Hill, U.S.A
mirali@med.unc.edu

Behrooz Masuodi
CT Division,
Dept. of Surgery
University of North Carolina, Chapel Hill, U.S.A
behroozmsd@gmail.com

Thomas Egan
Div. of Cardiothoracic Surgery,
Dept. of Surgery
University of North Carolina,
Chapel Hill, U.S.A
thomas_egan@email.unc.edu

Marie Muller
Dept. of Mechanical and Aerospace Engineering
NC State University,
Raleigh, U.S.A
mmuller2@ncsu.edu

***Abstract*—Ultrasound imaging in strongly heterogeneous media is challenging due to the aberrations caused by multiple scattering. The linearity between distance and time is lost making echolocation-based imaging elusive. In this study, we present a method for the imaging of anechoic lesions and targets in highly scattering media taking advantage of ultrasound multiple scattering. First, in silico, heterogeneous media are simulated with 10% area fraction of plastic scatterers in water. Circular lesion (areas with no scatterers) with diameter 8mm are placed at a depth of 10mm. Experimentally, a petroleum jelly lesion is placed in a sponge partially saturated with water, and in a pig lung ex vivo. Inter-elements Response Matrix are acquired using a tranducer array. The backscattered intensity is calculated and split into its coherent and incoherent parts. From the incoherent intensity, a diffusion map is generated and combined with a depression detection algorithm to predict the presence, location and size of the lesions.**

Keywords*—*multiple scattering, lesion detection, ultrasound imaging, random media, lung nodule, lung cancer

I. Introduction

Generating ultrasound images in biological tissue is based on the concept of echolocation. The distance and time are related by the speed of sound in the medium which has to be known a priori. This framework is well suited to homogeneous or weakly heterogeneous media, where single scattering can be assumed to dominate. However in the presence of a strong scatterers and high scatterer density, the ultrasound wave bounces off of the scatterers multiple times generating aberrations and complex speckle pattern. Multiple scattering plays a major role and the wave propagation regime shifts to the diffusion regime[1]. In these cases, classical imaging methods fail. Media with strong scatterers are characterized by high attenuation, loss of linearity between distance and time and dominance of multiple scattering over single scattering.

Rather than considering multiple scattering as an obstacle, it can be taken advantage of. By using multiple scattering signals, the diffusivity of the medium can be quantified using the diffusion constant (D) and further extract transport parameters of the disordered media such as transport and scattering mean paths [2]–[5]. Algorithms have been developed to characterize strongly scattering complex media. Aubry & Derode's [6] proposed a method for the separation and multiple and single scattering contributions in random media. The separation combined with DORT (decomposition of the time-reversal operator) has the ability to remove any multiple scattering contribution [7]. Shahjahan et al [8], [9] proposed to combine the DORT to a multiple scattering filter to detect cracks or notches in heterogeneous media. Previous work have demonstrated the applicability of extracting the incoherent intensity of the backscattered wave to calculate D and characterize disordered media such as bone, the lung parenchyma and melamine sponge foams [10-13] Mohanty et al [14] also showed that using smaller sections of an ultrasound linear array, one could map D along the transducer axis to detect heterogeneity in a porous medium and identify the presence of anechoic lesions in complex medium.

The aim of the present study is to provide an imaging algorithm capable of detecting and localizing lesions in highly scattering media by measuring local changes of the diffusion constant, reflected by local changes in the rate of growth of the diffusive halo. In the presence of strong scatterers such as plastic scatterers in water, if the a lesion is placed at a distance larger than the scattering mean free path, traditional imaging fails[8]. By measuring local changes in the rate of spatial spread of the incoherent intensity, one can detect local fluctuations in D and

National Institutes of Health, R21CA231503. TE was supported by the UNC Lung Transplant Research Fund with generous contributions from the Ferguson family and John Doherty

detect the location and size of a lesion. A depression detection filter previously developed by Winslow et al. [15] can then be applied to identify the regions and spatial extent of the depression, thereby giving an estimate of the location and size of the lesion. We first demonstrate the proof-of concept in simulations where plastic scatterers are placed in water with an area fraction of (AF) 10% . The target to be imaged is an anechoic lesion (a region of absence of scatterers) whose size and depth are 8mm and 10mm respectively. We then show that it is feasible experimentally in a sponge phantom and in a pig lung ex vivo containing petroleum jelly lesions.

II. Materials and Methods

A. Data Acquisition

An Inter-Element Response Matrix (IRM) is acquired using an N element linear array transducer (N=128, Verasonics L7-4). The transducer is placed in the near-field and 2 cycle Gaussian pulses with central frequency 5MHz were transmitted consecutively from each of the transducer elements i and received by all receivers j=1:N for every transmit. The IRM is represented by $H(t)$ whose dimensions are N*N*t , the individual elements of which are $h_{ij}(t)$[5], [11], [12]. Once the IRM is obtained, it is split into sub-IRMs $H_z(t)$ containing only 43 elements.This is also described in *Figure 1.*

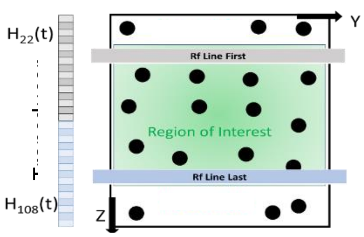

Figure 1:Splitting the IRM into sub-IRMs

B. Mapping the spread of the diffusive halo

The backscattered intensity for each sub-IRM $H_z(t)$ is calculated by appropriately time shifting the signal and truncating it over 0.4 µs overlapping windows, and then integrating the squared value of the signals over the appropriate time windows [5], [11], [16].

$$I_{ij}^z(T) = \int_{T-t/2}^{T+t/2} \left(h_{ij}^z(t)\right)^2 dt \qquad (2)$$

Where T is the time window number and t is the time window length t = [1µs]. $I_{inc}(X,T)$ is a 2D intensity matrix and is a function of T and X=|i-j|. For each sub-IRM, $H_z(t)$, the incoherent backscattered intensity can be expressed as a function of the diffusion constant D_z according to

$$I_{inc}^z(X,T) = I^z(X,T)\exp\left(-\frac{X^2}{4D_zT}\right) \qquad (1)$$

Where X represents the distance between emitter and receiver and D_Z is the semi-local diffusion constant. [11], [12]. At each time window, the incoherent intensity profile is fitted with a Gaussian curve(Eq.1) and its variance (W_z^2 (T) =$2D_zT$) [11], [16] is plotted against time. This is repeated for all sub-IRM positions z to obtain a 2D variance map which is denoted by W^2(z,T). The time is converted into depth by associating T with the depth of propagation using an arbitrarily defined speed of sound C_{eff}. This leads to the formulation of a final 2D variance map denoted by W^2(z,y) where z represents the transducer axis and y represents the depth in the medium. The 2D variance map here denotes the local changes in the growth of the diffusive halo.

C. Image Processing

As the wave enters the region without scatterers, the diffusion constant increases abruptly and so does the slope of the variance curve [11], [12], [14], [17]. The localized increase in the variance is what enables us to track the location of the anechoic lesion by tracking local fluctuations in the diffusion constant D. To identify the location of this rapid change, these deviations from a linear behavior are treated as outliers and isolated. To do so, we define two new matrices or 2D fields.

1. Linear Fit Field (L (z,y)) : Map generated from a line by line, linear regression fit of W^2(z,y).
2. Delta Field (Δ(z,y)): Map showcasing potential outliers in the variance map.

$$\Delta(z,y) = 1 - \mathrm{abs}\left(W^2(z,y) - L(z,y)\right) \qquad (3)$$

The delta field is a representation of the outlier map. In an ideal case, the outliers will form a closed enclosure, which needs to be extracted in order to map the anechoic lesion. The delta map is first treated with a 2-D median filter. Then, we apply a Depression Detection Filter, based on the work by Winslow et al [15]. The filter treats the outside edges of the closed loop depression as the edges and the depth of the depression is also evaluated. A binary threshold is then applied to isolate the lesion and represents its location. A normal Gaussian filter of order 4 is applied in order to obtain an estimate of the actual size of the lesion.

D. Numerical Simulation

Finite difference time-domain (FDTD) simulations are conducted using Simsonic [18]. Heterogeneous structures of area fractions (AF) 10% and lesion size of 8mm placed at a depth of 10mm are generated using a Monte Carlo method. Given in *Figure 2* is an example of such a structure used in simulation. The scatterer size (300µm, comparable to the wavelength) and the impedance difference between the scatterer and the propagation medium ensure a strongly scattering regime. A water layer 3 mm thick was simulated between the ultrasound probe and the heterogeneous medium to simulate ultrasound coupling gel.

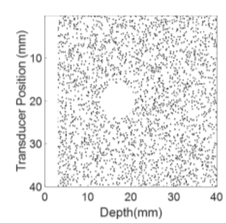

Figure 2: Simulation domain

The image shown in *Figure 2* is binary. The white portion is treated as water (density = 1000kg/m^3 and speed of sound = 1500 mm/µs) and the circular scatterers (diameter = 300 µm) are given properties of plastic (density = 1215 kg/ m^3 and speed of sound

2.25 mm/µs). The dimensions of the structure are 40 x 40 mm. The grid step for the numerical simulation is *dx* = 0.02mm and the time step is *dt* = 0.0022 µs.

E. Lesion in air saturated media

1 ml of petroleum jelly is injected using an 11 gauge needle in a sponge partially saturated with water. The air volume fraction in the sponge is evaluated by wx eighing the sponge and is estimated at 10% volume fraction. After ultrasound acquisition, the sponge is cut at the location of the Vaseline nodule. The diameter of the nodule is approximately 10 mm. The lesion appears to be circular. Similarly, a Vaseline nodule is injected in an ex-vivo pig lung partially inflated using an Ambu bag and an endotracheal tube.

III. Results and Discussion

The normalized variance field was fitted with a linear regression model, line by line, to obtain the linear fit. Once the delta field was obtained, the nodule location was isolated. After the application of the depression detection filter, the image obtained should contain only the lesion. However due to large amounts of multiple scattering, the depression detection filter detects not only the lesions but other closed loop. These false positive lesions were eliminated using a threshold.

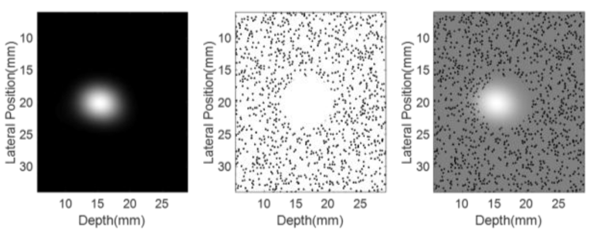

Figure 3: Results for lesion detection in silico

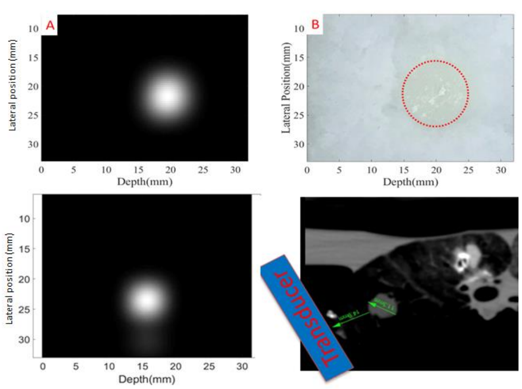

Figure 4: Results for lesion detection in a sponge phantom (top) and in a partially inflated pig lung ex vivo (bottom).

Shown in Figure 3 are results obtained for the 8mm lesion size for 10% AF with the defect located at 10 mm depth. Fig. 4 shows results obtained for approximately 10 mm Vaseline lesions in a sponge and in an inflated pig lung ex vivo. A good agreement is found between the true and predicted lesions sizes. The signal to noise ratio was calculated after the depression detection phase and before applying the threshold to isolate the lesion. All false positive lesions were treated as noise.

$$SNR = 20\log(\frac{I_{lesion}^{max}}{I_{noise}^{max}}) \qquad (4)$$

The SNR was found to be 7.2dB for the lesion detection in simulation, 2.4dB for the Vaseline lesion detection in the sponge, and 1.3dB for the Vaseline lesion detection in the pug lung ex vivo. A slight offset in the depth of the reconstructed lesions can be observed, which is attributed to the arbitrary choice of speed of effective sound. In the future, the effective speed of sound could potentially be tabulated in the lung as a function of inflation, but this remains to be investigated and.

However, this method seems to show promise in predicting the location and size of a lesion. We use the multiple backscattered signal to calculate the spatial growth incoherent backscattered intensity as a function of time/depth. When the wave propagates back after interacting with a lesion/target, due to the presence of scatterers on its backtracked path, it loses some of the information. This is a major obstacle in imaging any media with dense populations of strong scatterers. The main purpose of this algorithm was to propose a unified methodology to detect lesions as well as targets. We defined a lesion as a region with no scatterers whereas a target as a much larger scatterer. In more realistic applications, the lesion will not be perfectly homogeneous and will contribute to backscattererd intensities but those backscattering signals would be negligible compared to the multiple backscattering contributions due to plastic scatterers.

IV. Conclusion

The goal of this work was to develop a method for detection and localization of targets and lesions embedded in highly scattering heterogeneous media. It relies on the acquisition of IRMs, which is split into smaller sub-IRMs. The backscattererd incoherent intensity is mapped and local deviations in the linear growth of the diffusive halo over time allows imaging lesions and targets. This algorithm was able to detect lesions with high fidelity by locally tracking the changes in the variance. The combination of a DDF and diffusive halo 2-D map allowed for the prediction of the lesion location as well as the size with high accuracies. This algorithm could potentially be used to detect solitary pulmonary nodules by mapping the local deviations in variance.

References

[1] Z. Q. Zhang, I. P. Jones, H. P. Schriemer, J. H. Page, D. a Weitz, and P. Sheng, "Wave transport in random media: the ballistic to diffusive transition.," *Phys. Rev. E. Stat. Phys. Plasmas. Fluids. Relat. Interdiscip. Topics*, vol. 60, no. 4 Pt B, pp. 4843–4850, 1999.

[2] H. Schriemer, M. Cowan, J. Page, P. Sheng, Z. Liu, and D. Weitz, "Energy Velocity of Diffusing Waves in Strongly Scattering Media," *Phys. Rev. Lett.*, vol. 79, no. 17, pp. 3166–3169, 1997.

[3] M. L. Cowan, K. Beaty, J. H. Page, Z. Liu, and P. Sheng, "Group velocity of acoustic waves in strongly scattering media: Dependence on the volume fraction of scatterers," *Phys. Rev. E*, vol. 58, no. 5, pp. 6626–6636, 1998.

[4] J. H. Page, I. P. Jones, H. P. Schriemer, M. L. Cowan, P. Sheng, and D. A. Weitz, "Diffusive transport of acoustic waves in stronogly scattering media," *Physica B*, vol. 263–264. pp. 37–39, 1999.

[5] A. Tourin, A. Derode, A. Peyre, and M. Fink, "Transport parameters for an ultrasonic pulsed wave propagating in a multiple scattering medium," *J. Acoust. Soc. Am.*, vol. 108, no. 2, p. 503, 2000.

[6] A. Aubry and A. Derode, "Multiple scattering of ultrasound in weakly inhomogeneous media: Application to human soft tissues," *J.*

Acoust. Soc. Am., vol. 129, no. 1, p. 225, 2011.

[7] A. Aubry and A. Derode, "Detection and imaging in a random medium: A matrix method to overcome multiple scattering and aberration," *J. Appl. Phys.*, vol. 106, no. 4, pp. 1–48, 2009.

[8] S. Shahjahan, A. Aubry, F. Rupin, B. Chassignole, and A. Derode, "Improvement of Flaw Detection with Ultrasonic Array Probes in Multiple Scattering Polycrystalline Materials by Means of a Random Matrix Approach," no. May, pp. 20–24, 2013.

[9] S. Shahjahan, F. Rupin, A. Aubry, and A. Derode, "Evaluation of a multiple scattering filter to enhance defect detection in heterogeneous media," *J. Acoust. Soc. Am.*, vol. 141, no. 1, pp. 624–640, 2017.

[10] Karbalaeisadegh, Y., Yousefian, O., Iori, G., Raum, K., & Muller, M. (2019). Acoustic diffusion constant of cortical bone: Numerical simulation study of the effect of pore size and pore density on multiple scattering. *The Journal of the Acoustical Society of America*, *146*(2), 1015-1023.

[11] A. Aubry and A. Derode, "Ultrasonic imaging of highly scattering media from local measurements of the diffusion constant: Separation of coherent and incoherent intensities," *Phys. Rev. E - Stat. Nonlinear, Soft Matter Phys.*, vol. 75, no. 2, pp. 1–9, 2007.

[12] K. Mohanty, J. Blackwell, T. Egan, and M. Muller, "Characterization of the Lung Parenchyma Using Ultrasound Multiple Scattering," *Ultrasound Med. Biol.*, vol. 43, no. 5, pp. 993–1003, May 2017.

[13] H. Du, K. Mohanty, and M. Muller, "Microstructural characterization of trabecular bone using ultrasonic backscattering and diffusion parameters," *J. Acoust. Soc. Am.*, vol. 141, no. 5, pp. EL445-EL451, 2017

[14] K. Mohanty, J. Blackwell, S. B. Masuodi, M. H. Ali, T. Egan, and M. Muller, "1-Dimensional quantitative micro-architecture mapping of multiple scattering media using backscattering of ultrasound in the near-field: Application to nodule imaging in the lungs," *Appl. Phys. Lett.*, 2018.

[15] L. A. Winslow, "Landscape Limnology: Lake morphology and process at the continental scale," UNIVERSITY OF WISCONSIN – MADISON, 2014.

[16] A. Aubry, A. Derode, and F. Padilla, "Local measurements of the diffusion constant in multiple scattering media: Application to human trabecular bone imaging," *J. Acoust. Soc. Am.*, vol. 123, no. 5, p. 3633, 2008.

[17] A. Derode, V. Mamou, F. Padilla, F. Jenson, and P. Laugier, "Dynamic coherent backscattering in a heterogeneous absorbing medium: Application to human trabecular bone characterization," *Appl. Phys. Lett.*, vol. 87, no. 11, pp. 1–3, 2005.

[18] E. Bossy, M. Talmant, and P. Laugier, "Three-dimensional simulations of ultrasonic axial transmission velocity measurement on cortical bone models," *J. Acoust. Soc. Am.*, vol. 115, no. 5, pp. 2314–2324, 2004.